Whole-rock Major- and Trace-element Chemistry of 1992 Ejecta from Crater Peak, Mount Spurr Volcano, Alaska

By Christopher J. Nye, Michelle L. Harbin, Thomas P. Miller, Samuel E. Swanson, and Christina A. Neal

CONTENTS

ABSTRACT

Juvenile ejecta from the three 1992 eruptions of the Crater Peak vent of Mount Spurr are calcalkaline andesite and contain about 57 percent SiO_2 by weight. Samples are chemically uniform within analytical error for all but a few of the most mobile of the 43 elements whose concentrations were determined. The andesite is unlike prehistoric Crater Peak andesites of similar silica content in having high concentrations of Al_2O_3, Na_2O, and Sr and low concentrations of compatible transition metals. These differences suggest that the immediate parent to the 1992 andesite crystallized relatively more ferromagnesian silicate (probably clinopyroxene) and less plagioclase than previous Mount Spurr andesites, which requires either higher water pressure, greater residence depth, or both. The 1992 andesite is also unlike previous Crater Peak andesites, including that erupted in 1953, in having lower concentrations of some incompatible elements yet higher amounts of silica. These observations suggest that the magma that fed the 1992 eruptions was not derived from the same magma body that fed the 1953 eruption, but it instead is new magma that came from the source region in the deepest crust or mantle. The 1992 eruptions also ejected partially melted aluminous metamorphic xenoliths characterized by high concentrations of both incompatible and compatible trace elements despite moderate silica contents and by mineral assemblages unlike exposed country rock. Small quantities of highly siliceous xenoliths characterized by dramatic depletion of all but a few trace elements (Rb, Ta, U) were also erupted.

INTRODUCTION

Mount Spurr volcano, 125 km west of Anchorage, is the next-to-last Holocene volcano at the northeastern end of the Aleutian arc. It is about 100 km above the Benioff zone and 500 km from the trench in a direction parallel to the movement between the Pacific and North American plates. The region surrounding Mount Spurr is underlain by a Jurassic to mid-Tertiary granitic batholith, which intrudes Paleozoic to Mesozoic limestone, basalt, and flysch of generally low metamorphic grade (Wilson and others, 1985).

Spurr volcano is composed of an ancestral Mount Spurr (fig. 1) whose construction began at least 255 ka (Nye and Turner, 1990). It is predominantly built of 58 to 60 percent SiO_2 two-pyroxene andesite flows that are interbedded with a few more mafic flows. Lava flows dominate the upper part of the cone, and pyroclastic rocks dominate the lower part. The growth of the ancestral Mount Spurr was terminated by Bezymianny-type avalanche caldera formation and the production of a debris avalanche with a minimum runout of 25 km and a volume of a few cubic kilometers (Nye and Turner, 1990). The resultant amphitheater is 5 km by 6 km, predominantly ice filled, and breached to the south. The debris avalanche is immediately overlain by partially welded ashflows more silicic (61–63 percent SiO_2) than ancestral Mount Spurr andesites. Intrusion of this silicic magma high into the cone was presumably the cause of stratocone failure. The age of caldera formation is not precisely known. It post-

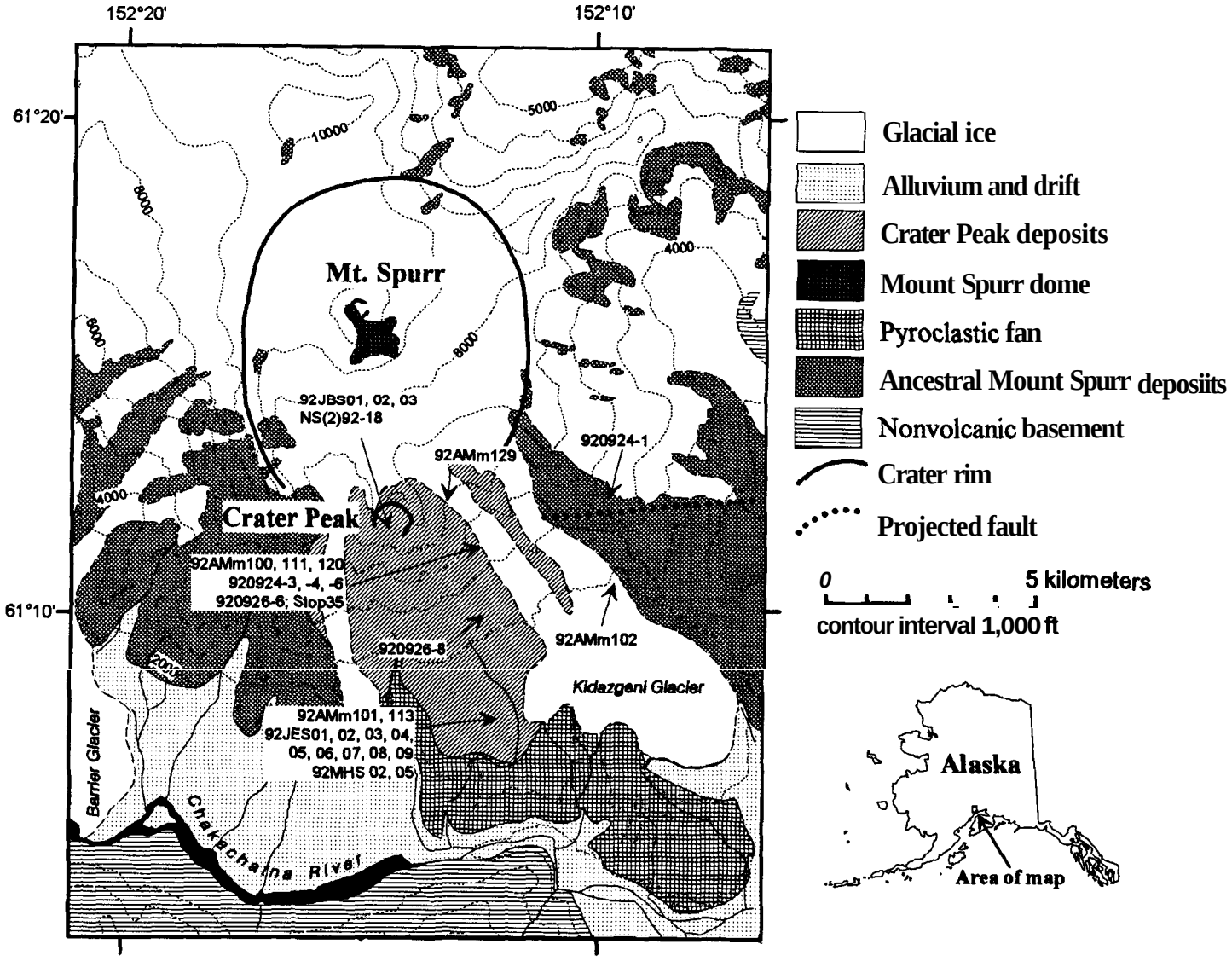

Figure 1. Geology (modified Nye and Turner, 1990) and geography of the area immediately surrounding Mount Spurr, Alaska. Locations of samples analyzed for this study are also shown.

dates the youngest cone-building andesite (youngest measured age is 59 ka; Nye and Turner, 1990) and predates the oldest post-caldera tephra (>7 ka; Riehle, 1985). The lack of a tephra blanket suggests that caldera formation occurred during a time of widespread ice cover, ergo a Pleistocene age. The lack of erosion of the debris avalanche, despite its location in major glacial valley, suggests a late Pleistocene age of caldera formation.

After caldera formation, a large dome formed in the center of the caldera (fig. 1). It forms the current summit of Mount Spurr and is ice covered except for periodically exposed patches of dome lava with scattered, diffuse boiling-point fumaroles. The few samples recovered from the dome have 61 to 63 weight percent SiO_2, plagioclase, two pyroxenes, and occasional hornblende xenocrysts and have compositions similar to the ashflows overlying the debris avalanche (Nye and Turner, 1990). Tephra from this vent do not appear to be younger than about 5 ka (Riehle, 1985). Crater Peak, 6 km south of the Mount Spurr summit (fig. 1), sits in the caldera breach and is the historically active vent. It consists of lava and pyroclastic flows with 54 to 57 percent SiO_2—more mafic than cone-building andesites, which contain plagioclase, two pyroxenes, and sparse hornblende phenocrysts. Tephra from Crater Peak range in age from 5 ka to the present (Riehle, 1985). However, the presence of block-and-ash flows produced by the eruption of magmas that are apparent mixtures of Crater Peak and Spurr summit dome magmas as well as hornblende xenocrysts derived from Crater Peak magmas in Spurr summit dome magmas, suggest that the two magmatic systems overlapped in time (Nye and Turner,

1990). Remnants of an older cone in the position of the current Crater Peak lie just west and east of Crater Peak. These are referred to as ancestral Crater Peak here, but they were called proto-Crater Peak by Nye and Turner (1990).

The Crater Peak vent of Mount Spurr erupted on June 27, August 18, and September 16–17, 1992 (Eichelberger and others, this volume). Eruptions were 3.5 to 4 hours in duration, and they produced subplinian columns which deposited extensive tephra blankets and minor proximal pyroclastic flows and other debris flows. These eruptions produced six types of ejecta. In order of decreasing volume, they are: (1) widespread blankets of mostly juvenile andesitic tephra with a combined dense-rock-equivalent volume of about 35x106 m3 (Neal and others, this volume); (2) brown to dark-gray, breadcrusted andesite blocks deposited in pyroclastic flows, lahars, and ballistic bomb fields with a total volume of about one percent of that of the tephra (Miller and others, this volume; Waitt and others, this volume); (3) aluminous xenoliths composed of highly inflated, partially melted blocks of metamorphic country rock, with a total volume of about one percent of the volume of the andesite blocks (Harbin and others, this volume); (4) light gray-green andesite, which is distinguished most readily from the dark andesite by clear, rhyolitic groundmass glass rather than the brown, andesitic glass of the dark andesite; (5) volumetrically minor metamorphic xenoliths including a white glass-quartz-plagioclase rock and wollastonite-bearing skarn; and (6) accidental blocks of older Crater Peak andesite. Representative samples of most of these types of ejecta were analyzed in bulk for 10 major and 33 trace elements.

ACKNOWLEDGMENTS

We thank Diane Johnson and Charles Knaack of the GeoAnalytical Laboratory at Washington State University for their fast, courteous, and responsive attention to our analytical requests. We also thank members of the Alaska Volcano Observatory and its affiliates including Jim Beget, John Eichelberger, and Cynthia Gardner for collecting some of the samples for this study. Julie Donnelly-Nolan and John Pallister provided conscientious technical reviews that substantially improved the original manuscript.

SAMPLE SUITE AND ANALYTICAL QUALITY

The samples discussed herein include 19 juvenile andesite blocks (three from the June 27 eruption, nine from the August 18 eruption, and seven from the September 16–17 eruption). These blocks span the known emplacement modes and stages of each eruption. We also analyzed five light gray-green andesites (four from August 18 and one 1 from September 16–17); 20 aluminous xenoliths (all from August 18); and 3 white glass-quartz-plagioclase xenoliths from August 18 deposits. Sample locations for andesite blocks and xenoliths are shown in figure 1. In addition we analyzed a total of 20 proximal tephra samples consisting of two or three samples from light and dark and upper and lower tephra from each eruption. These are described more fully in Neal and others (this volume). Separate splits of each sample were powdered in a tungsten-carbide shatterbox for analysis by X-ray fluorescence (XRF) and in a steel shatterbox for analysis by inductively coupled plasma mass spectrometry (ICP/MS). Crushing in tungsten-carbide avoids compatible-transition-metal contamination and crushing in steel prevents high-field-strength element contamination. Milling and analysis were done at the GeoAnalytical laboratory at Washington State University. One duplicate was chosen at random and analyzed for each batch of samples submitted. These duplicates form the basis for our reported analytical precision (table 1). Overlap of analyzed elements between techniques (high-precision Rb, Ba, Y, and Nb data were obtained by both XRF and ICP-MS) provides another method of monitoring analytical quality.

ANDESITE

HOMOGENEITY OF 1992 ANDESITE

Two types of andesite erupted from Crater Peak in 1992: dense to scoriaceous brown to dark-gray andesite and much less abundant light gray-green andesite. The dark andesite is fairly homogeneous throughout the deposits from all three 1992 eruptions (tables 1, 2). For most elements the percent deviation of all 1992 Spurr andesites is close to the analytical precision of the laboratory. Some of the highly incompatible elements (Cs, Rb, U, Th, and Pb) have variations in 1992 ejecta outside analytical precision, but even for these elements the total variation among samples is small. For example, Cs variability between samples is about 9 percent, but this only represents a 0.04-ppm standard deviation of the analyses. Pb variability is apparently quite high (18 percent), but this reflects the inclusion in the mean of a single sample from the September 17 eruption with 9.54 ppm Pb. Omission of this sample from the calculation results in a relative deviation of only 4 percent. We did not analyzed this sample in duplicate to verify its Pb content. Some of the compatible transition metals (Fe, Sc, Cr, and Ni) also show variability outside analytical precision.

Table 1. Whole-rock composition of selected historic and prehistoric andesites erupted from the Crater Peak vent of Mount Spun, Alaska.

[Sample locations, modes and descriptions for samples not described herein given by in Nye and Turner (1990). Mean for dark 1992 andesite is for 19 juvniile andesite blocks from 1992 eruptions of Crater Peak; std dev., one standard deviations of the analyses in preceding column; % dev. is the standard deviation expressed as a percentage of the mean for each element; precision refers to analytical precision, in percent, of these analyses as indicated by duplicate studies. Major elements normalized to 100 percent anhydrous. FeOt is total iron as FeO. Number of reported decimal places may exceed analytical precision.]

	Prehistoric Crater Peak andesite				1953 andesite		Dark 1992 andesite				Liaht grey-green 1992 andesite				
Sample	PCP-801	PCP-A02	CP-02	CP-12	PUM-16	PUM-17	mean	std. dev.	%dev.	precision (20)	92AMm 102GS	92AMm 113C	92JES -01	92MHS 10	92AMm 120A
Maior-element oxides, in weiaht percent															
SiO_2	57.44	56.61	56.61	56.30	54.89	54.35	56.73	0.34	0.6	0.2	56.59	58.84	56.47	56.16	56.52
	0.85	0.79	0.87	0.79	0.86	0.91	0.69	0.01	1.2	1.2	0.67	0.64	0.70	0.76	0.71
Al_2O_3	17.23	17.14	18.00	18.55	18.80	18.61	19.05	0.11	0.6	0.6	19.33	18.23	18.95	18.77	19.02
FeOt	6.91	7.00	7.05	6.99	7.68	7.68	6.95	0.29	4.2	1.6	6.82	6.53	7.10	7.39	7.07
MnO	0.14	0.14	0.14	0.14	0.15	0.14	0.15	0.00	1.7	1.2	0.15	0.14	0.16	0.16	0.15
MgO	5.04	6.33	4.61	4.32	4.58	4.85	3.65	0.07	1.9	1.2	3.52	3.46	3.75	3.93	3.74
CaO	7.54	7.59	7.38	7.38	8.02	8.14	7.57	0.08	1.0	0.8	7.65	6.69	7.74	7.91	7.61
Na_2O	3.41	3.25	3.85	4.21	3.81	4.07	4.02	0.07	1.8	1.0	4.08	4.10	3.92	3.77	3.98
K_2O	1.24	0.95	1.25	1.05	0.95	0.99	0.91	0.03	2.8	1.4	0.90	1.14	0.93	0.88	0.93
P_2O_5	0.21	0.19	0.25	0.26	0.26	0.26	0.28	0.01	4.8	0.6	0.29	0.23	0.28	0.28	0.28
Trace elements. in parts per million															
Cs	0.17	0.14	0.28	0.22	0.60	0.19	0.45	0.05	10.0	2	0.57	0.41	0.83	0.53	0.51
Rb	26.96	19.79	29.82	21.85	16.70	18.53	15.12	1.20	7.9	2	15.56	18.04	15.44	14.57	18.39
Ba	459.53	453.07	448.69	358.99	385.17	357.34	385.24	8.81	2.3	1	397.00	411.78	387.39	352.53	381.20
Sr	558.00	554.00	612.00	681.00	620.00	699.00	658.84	8.76	1.3	1	671.00	564.00	657.00	629.00	650.00
La	13.82	11.32	14.79	10.01	11.12	12.10	11.05	0.25	2.2	4	11.46	11.28	11.02	10.30	10.76
Ce	28.04	22.56	29.67	21.60	22.89	24.86	22.63	0.55	2.4	4	23.87	22.04	22.59	21.47	21.65
Pr	3.56	2.84	3.74	2.82	3.03	3.26	2.96	0.06	2.1	4	3.15	2.82	2.84	2.88	2.93
Nd	15.53	12.60	16.39	12.71	13.64	14.68	13.24	0.32	2.5	4	13.93	12.23	12.87	12.83	12.94
Sm	3.72	3.26	4.13	3.22	3.67	3.71	3.33	0.09	2.7	4	3.51	3.06	3.21	3.43	3.23
Eu	1.18	1.14	1.27	1.06	1.26	1.26	1.14	0.04	3.5	4	1.23	0.98	1.08	1.17	1.12
Gd	3.51	3.12	3.62	2.80	3.38	3.30	3.08	0.09	3.1	4	3.06	2.82	2.98	3.30	2.91
Tb	0.58	0.50	0.61	0.48	0.57	0.55	0.51	0.01	2.3	4	0.52	0.48	0.51	0.55	0.51
Dy	3.53	3.08	3.58	2.87	3.36	3.30	3.09	0.07	2.3	4	3.18	2.86	2.98	3.26	3.01
Ho	0.72	0.63	0.71	0.56	0.68	0.66	0.63	0.01	2.1	4	0.65	0.58	0.61	0.68	0.63
Er	2.05	1.77	1.99	1.54	1.95	1.87	1.81	0.06	3.3	3	1.88	1.68	1.81	1.90	1.76
Tm	0.28	0.24	0.27	0.21	0.27	0.26	0.25	0.01	3.0	4	0.25	0.23	0.25	0.26	0.25
Yb	1.78	1.49	1.76	1.27	1.68	1.61	1.64	0.05	2.8	4	1.69	1.53	1.59	1.71	1.58
Lu	0.28	0.24	0.27	0.20	0.27	0.25	0.26	0.01	3.7	4	0.28	0.25	0.25	0.28	0.26
Y	18.97	16.58	20.65	9.40	18.43	17.90	17.24	0.63	3.6	6	17.60	14.88	17.54	18.65	17.14
Zr	110.00	103.00	115.00	106.00	100.00	106.00	104.79	0.77	0.7	1	103.00	106.00	103.00	102.00	104.00
Hf	2.63	2.25	2.48	2.21	2.10	2.16	2.15	0.07	3.1	6	2.12	2.15	2.10	2.15	2.06
Nb	9.60	4.08	6.05	4.93	5.46	4.54	4.55	0.18	3.9	6	4.73	4.16	4.70	5.15	4.41
Ta	1.28	0.27	0.34	0.27	0.22	0.25	0.25	0.01	5.3	6	0.28	0.26	0.26	0.31	0.25
Pb	4.00	4.33	5.09	5.28	4.83	5.02	5.51	0.98	17.7	6	5.17	5.02	5.25	4.64	5.31
Th	2.24	1.31	2.17	0.29	1.01	1.04	0.85	0.06	7.2	6	0.89	1.35	0.90	0.80	0.89
U	0.55	0.32	0.59	0.36	0.35	0.37	0.26	0.02	7.5	6	0.26	0.39	0.28	0.25	0.28
Ga	17	18	17	20	19	19	20.37	1.46	7.2	12	21	18	18	21	19
Cu	28	55	33	49	53	67	48.16	3.98	8.3	14	44	59	50	58	44
Zn	76	80	88	85	83	86	90.26	8.56	9.5	6	91	87	95	82	92
V	205	190	202	173	213	222	153.00	9.08	5.9	6	156	150	169	168	154
Sc	29	28	27	27	22	30	15.16	2.03	13.4	10	16	17	19	16	17
Cr	88	198	69	26	32	43	22.53	9.58	42.5	10	89	29	28	33	23
Ni	21	83	25	22	15	23	9.53	2.46	25.8	16	16	15	11	16	11

Table 2. Whole-rock compositions of dark andesite from 1992 eruptions of Crater Peak vent of Mount Spurr, Alaska.

[Major elements normalized to 100 percent anhydrous. FeOt is total iron as FeO. Number of reported decimal places may exceed analytical precision.]

Sample	92JBS01	92JBS02	92JBS03	9209268	92amm 100	92amm 101	92amm 111B	92JES03	92JES-06	92JES-07	92JES-08	NS(2)92-18	920924-1	920924-3	920926-6	92AMm 1208	92AMm 120C	92AMm 129	Stop35
	June 27 eruption			Auaust 18 eruption									September 16-17 eruption						
	Major-element oxides, in weight percent																		
SiO_2	56.68	56.64	56.61	56.74	56.51	56.45	56.50	56.39	56.42	56.87	56.44	56.96	56.86	56.62	57.05	56.54	56.55	57.19	57.85
TiO_2	0.68	0.68	0.68	0.69	0.68	0.68	0.69	0.69	0.70	0.68	0.68	0.67	0.70	0.68	0.70	0.70	0.69	0.68	0.69
Al_2O_3	19.14	19.08	19.13	18.98	19.27	19.13	19.05	19.05	18.79	18.95	19.19	18.97	18.99	19.17	19.12	18.87	18.98	18.99	19.13
FeOt	6.97	7.03	7.01	7.07	6.91	7.07	7.12	7.10	7.40	6.93	6.93	6.93	6.93	7.02	6.59	7.23	7.13	6.78	5.93
MnO	0.15	0.15	0.15	0.15	0.15	0.15	0.15	0.15	0.16	0.15	0.15	0.15	0.15	0.15	0.15	0.16	0.15	0.15	0.15
MgO	3.56	3.58	3.54	3.67	3.58	3.62	3.65	3.70	3.59	3.64	3.69	3.60	3.77	3.66	3.72	3.81	3.69	3.59	3.65
CaO	7.64	7.59	7.61	7.58	7.58	7.58	7.60	7.64	7.79	7.57	7.63	7.49	7.51	7.58	7.55	7.52	7.56	7.43	7.44
Na_2O	4.03	4.06	4.09	3.94	4.12	4.14	4.05	4.09	3.95	4.04	4.08	4.03	3.89	3.94	3.92	3.95	4.05	3.97	3.95
K_2O	0.88	0.87	0.88	0.88	0.90	0.90	0.91	0.90	0.91	0.90	0.91	0.93	0.92	0.89	0.94	0.94	0.92	0.94	0.97
P_2O_5	0.29	0.29			0.30	0.29	0.28	0.29	0.29	0.28		0.28	0.28	0.30			0.28	0.28	0.24
	Trace elements, in parts per million																		
Cs	0.4	0.4	0.4	0.42	0.43	0.42	0.43	0.44	0.46	0.45	0.44	0.48	0.48	0.42	0.57	0.45	0.46	0.51	0.53
Rb	16.09	15.99	16.06	13.86	15.13	15.55	14.32	14.48	13.37	13.51	13.28	14.71	15.28	13.71	15.30	17.03	16.46	15.86	17.27
Ba	384	386	382	371	402	396	380	379	385	379	382	398	383	381	387	378	371	398	397
Sr	662	670	666	671	667	663	664	661	653	660	665	654	647	671	651	649	655	649	640
La	11.4	11.17	10.87	11.09	11.31	11.54	10.86	11.14	10.98	10.97	11.10	11.20	10.98	11.13	10.80	10.53	10.57	11.09	11.15
Ce	23.11	23.08	22.98	22.95	23.39	23.71	22.08	22.45	22.40	22.47	22.64	22.81	22.41	22.96	22.07	21.60	21.44	22.67	22.82
Pr	3.03	3.04	3.01	3.04	3.01	3.07	2.91	2.89	2.90	2.88	2.94	2.98	2.89	2.96	2.95	2.89	2.85	2.97	2.99
Nd	13.7	13.68	13.72	13.57	13.65	13.7	13.01	12.95	13.29	13.08	13.03	13.09	12.99	13.24	13.05	12.73	12.70	13.24	13.18
Sm	3.48	3.46	3.39	3.40	3.36	3.42	3.31	3.27	3.26	3.26	3.34	3.40	3.16	3.36	3.26	3.23	3.15	3.39	3.36
Eu	1.22	1.2	1.18	1.15	1.2	1.19	1.13	1.09	1.13	1.12	1.11	1.13	1.10	1.13	1.10	1.14	1.07	1.15	1.14
Gd	3.23	3.19	3.19	3.10	3.24	3.15	2.92	3.01	3.10	3.06	3.00	3.17	2.93	3.13	3.03	3.00	3.02	3.11	2.99
Tb	0.52	0.52	0.53	0.51	0.54	0.53	0.51	0.50	0.50	0.50	0.51	0.51	0.50	0.52	0.50	0.51	0.51	0.50	0.50
Dy	3.15	3.2	3.17	3.16	3.16	3.14	2.98	3.04	3.00	3.05	3.07	3.13	2.95	3.09	3.01	3.07	3.06	3.16	3.07
Ho	0.65	0.66	0.65	0.64	0.66	0.64	0.62	0.63	0.62	0.64	0.61	0.64	0.62	0.64	0.62	0.62	0.62	0.63	0.64
Er	1.87	1.96	1.86	1.81	1.86	1.88	1.80	1.81	1.75	1.72	1.78	1.82	1.79	1.79	1.72	1.72	1.78	1.82	1.80
Tm	0.26	0.27	0.26	0.26	0.25	0.26	0.24	0.25	0.25	0.25	0.24	0.26	0.25	0.26	0.24	0.24	0.25	0.25	0.25
Yb	1.71	1.75	1.65	1.64	1.69	1.71	1.60	1.65	1.61	1.64	1.64	1.64	1.58	1.65	1.60	1.58	1.59	1.63	1.65
Lu	0.27	0.28	0.27	0.26	0.28	0.28	0.27	0.27	0.26	0.27	0.26	0.26	0.25	0.26	0.26	0.25	0.25	0.26	0.26
Y	17.89	17.83	18.21	17.36	18	17.75	15.34	17.43	17.32	17.12	16.75	16.55	16.86	17.05	16.89	17.02	17.26	17.38	17.58
Zr	104	105	104	105	105	105	106	105	105	103	105	106	104	105	105	104	104	105	106
Hf	2.21	2.24	2.16	2.15	2.22	2.24	2.08	2.11	2.13	2.05	2.07	2.15	2.11	2.21	2.18	2.13	2.00	2.19	2.21
Nb	4.82	4.73	4.86	4.63	4.74	4.71	4.06	4.56	4.55	4.53	4.45	4.46	4.46	4.53	4.41	4.46	4.40	4.62	4.57
Ta	0.27	0.28	0.26	0.24	0.27	0.27	0.24	0.25	0.25	0.25	0.24	0.25	0.24	0.25	0.26	0.24	0.23	0.25	0.26
Pb	5.83	5.35	5.14	5.00	5.44	4.96	5.58	5.29	5.12	4.96	5.09	5.44	5.31	9.54	5.21	5.25	5.25	5.22	5.69
Th	0.83	0.81	0.8	0.82	0.91	0.83	0.86	0.90	0.79	0.77	0.74	0.82	0.92	0.79	0.88	0.87	0.85	0.95	0.98
U	0.26	0.25	0.25	0.25	0.27	0.26	0.26	0.25	0.23	0.23	0.21	0.25	0.28	0.24	0.26	0.27	0.27	0.28	0.29
Ga	20	18	21	19	20	19	20	20	22	22	19	22	23	21	20	22	19	22	18
Cu	45	54	57	49	49	50	51	50	51	46	44	41	49	50	48	46	46	49	40
Zn	84	91	92	81	91	88	95	90	91	93	96	94	101	84	68	96	85	111	84
V	135	150	138	165	161	141	160	154	150	147	147	142	159	163	166	161	156	158	154
Sc	17	18	16	12	16	16	18	15	16	14	14	16	15	17	15	14	11	11	17
Cr	17	19	19	14	16	16	21	23	17	22	22	59	30	16	30	23	19	23	22
Ni	8	9	6	9	6	10	8	11	8	9	8	17	13	8	10	10	9	12	10

Four of the five light gray-green andesites that were analyzed are compositionally identical to the dark andesite, except for slightly higher and more variable Cs (table 1). This similarity is remarkable in view of the drastically different composition of the groundmass glass in the light gray-green andesites (rhyolite glass) versus dark andesites (andesite to dacite glass) (Harbin and others, this volume). The similar whole-rock chemistry in spite of different groundmass chemistry presumably reflects, on the scale of individual blocks, more extensive crystallization of the dark andesite to produce the light gray-green andesite, perhaps at the chamber margin. The fifth sample (92AMm113c) is more evolved, and it contains 58.8 percent SiO_2. This sample has no distinguishing petrographic characteristics, and it may contain a higher ratio of glass to crystals.

COMPARISON TO PREHISTORIC CRATER PEAK MAGMAS

Prehistoric Crater Peak lavas are hornblende-bearing two-pyroxene calcalkaline basaltic andesite and andesite (Nye and Turner, 1990). Besides being slightly more mafic than all but a very few ancestral cone-building andesites, their most important distinguishing feature compared to other Mount Spurr lavas is the presence of centimeter-sized, holocrystalline, cumulus pyroxenite clots (Nye and Turner, 1990). The 1992 magma is also calcalkaline andesite, but it falls outside chemical trends of prehistoric magmas in many ways. The 1953 and prehistoric lava compositions normalized to average 1992 andesite are shown in figure 2. Data for selected samples are presented in table 1. The prehistoric andesites that are plotted have SiO_2 within 1 weight percent of the 1992 andesite. Important differences between the 1992 andesite and previous andesites, at nearly constant SiO_2, are higher concentrations of Al, Na, and Sr, and lower concentrations of Ti, V, Mg, Sc, Cr, and Ni. These two observations suggest more protracted crystallization of the parent to the 1992 andesite at mid- to lower-crustal depths, where the increased pressure favors ferromagnesian silicate crystallization over plagioclase crystallization. MgO and Al_2O_3 versus SiO_2 are shown in figure 3 for the entire Mount Spurr suite. These plots suggest that increased plagioclase (high Al_2O_3) and decreased pyroxene (low MgO) components in the 1992 andesites are shared by the 1953 andesites, but not by most older magmas. Low MgO by itself does not uniquely demonstrate pyroxene crystallization, but pyroxene is likely to be the most abundant ferromagnesian phase. Greater-than-normal reservoir depths may be characteristic of latest Holocene Crater Peak magmatism.

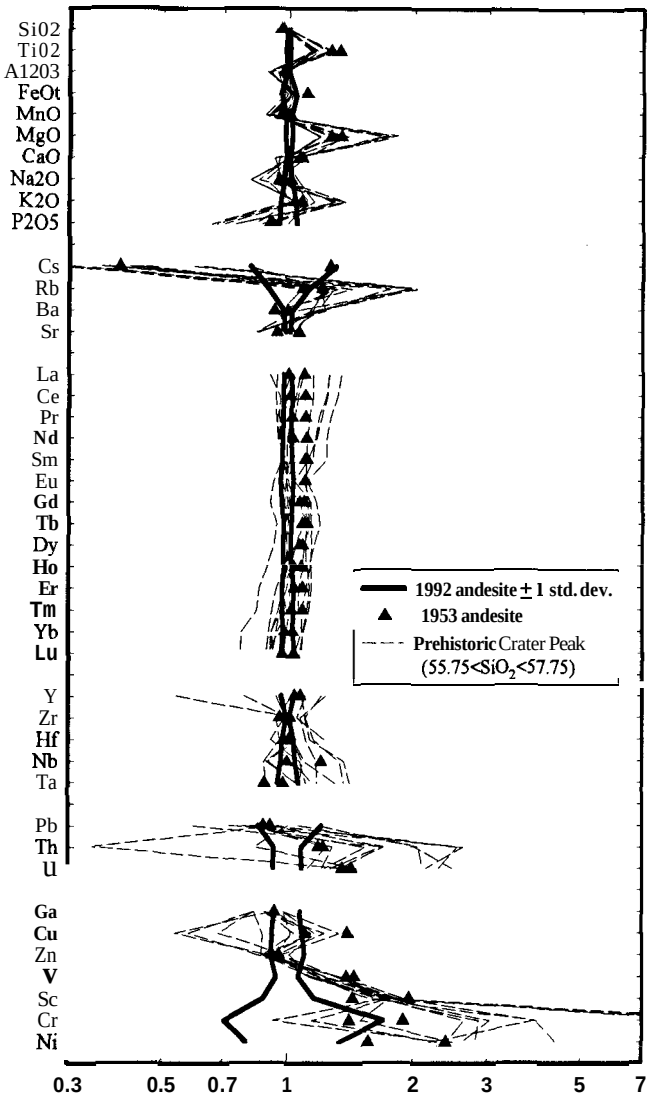

Figure 2. Mean composition of andesite erupted during 1992 from Crater Peak volcano, Mount Spurr, Alaska, compared to 1953 andesite and prehistoric Crater Peak andesite. Each line is a single sample's composition divided by the mean composition of 1992 andesite blocks. Gaps separate groups of geochemically similar elements. FeO_t is total iron as FeO.

There are also major differences in the abundances and ratios of highly incompatible trace elements between 1992 andesite and previous andesite of similar SiO_2. Specifically, 1992 andesite has Cs concentrations about two times higher than older andesite, yet slightly lower concentrations of the other alkali elements K and Rb. These differences are about 20 times analytical uncertainty. Compared to most previous andesite, 1992 andesite has low concentrations of Th and U, yet it has about the same Pb content. These differences in the relative concentrations of

highly incompatible elements cannot be generated by fractional crystallization and must reflect some process in the source that varies for individual batches of magma. Andesite from the 1992 eruptions has a slightly lower La/Yb ratio, and thus it is slightly less light-rare-earth-element enriched than previous andesite. Concentrations of the high-field-strength elements are comparable for some, but not all, samples of previous Crater Peak andesite.

Rb-SiO_2 variations in samples from the 1992 and 1953 eruptions of Crater Peak are shown in figure 4; also shown are Rb-SiO_2 variations from prehistoric flows from Crater Peak and the eastern and western remnants of the ancestral Crater Peak. The relative stratigraphic positions of samples are known, with the exception that the relative ages of the east and west ancestral Crater Peak sections are unknown. Three groups of samples (Crater Peak and west and east ancestral Crater Peak) are connected by lines in order of stratigraphic succession. In each case the oldest samples are the most silicic. In many cases Rb variations in near-neighbor mafic flows are so large that they cannot be related by fractional crystallization or mixing. Rb variations at 54 to 55 percent SiO_2 are large enough that simple crystal sorting also cannot explain the variations. These relations suggest that relatively small volumes of chemically unrelated magma can migrate from deep within the system to feed just a few eruptions.

COMPARISON TO 1953 MAGMA

An important volcanological question is whether the 1992 andesite erupted from new magma that recently migrated to the upper crust, or whether it erupted from the remnant of the upper-crustal magma body that fed the 1953 eruption. Analyses of two samples from proximal 1953 pumice deposits are shown in table 1 and plotted in figures 2, 3, and 4. Andesite from 1992 is unlike 1953 andesite in that, despite its higher SiO_2, it has lower concentrations of some incompatible elements such as Rb, U, and the middle rare-earth elements. These differences cannot be produced by fractional crystallization, and they suggest that the 1992 andesite indeed represents a new magma. Calculated fractional crystallization paths for 1953 magmas are shown in figure 4. The crystallization calculation is from Nye and Turner (1990) and is based on detailed least-squares calculations to relate SiO_2 in-

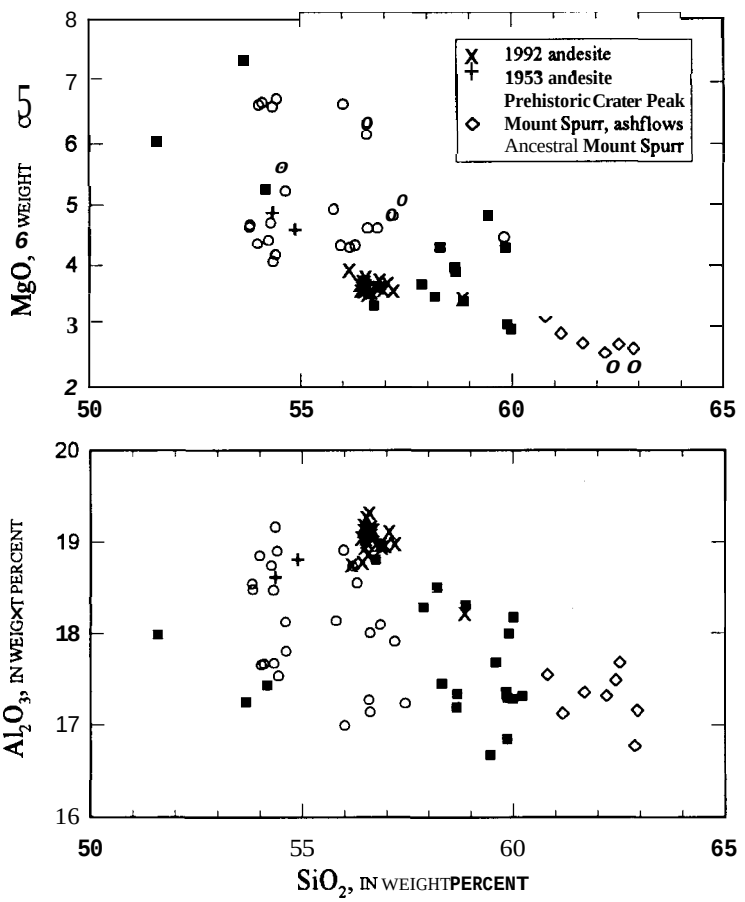

Figure 3. MgO and Al_2O_3 versus SiO_2 (in weight percent) of Pleistocene, Holocene, and historic samples from Mount Spurr volcano, Alaska. Samples not discussed in this paper are discussed in Nye and Turner (1990). Note the high Al_2O_3 and low MgO of 1992 andesite compared to previous Crater Peak andesite and other Mount Spurr lavas.

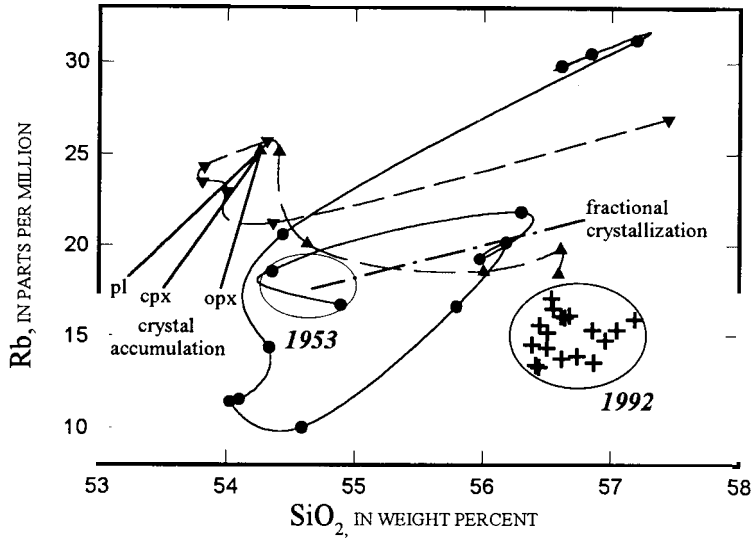

Figure 4. Rb (in ppm) versus SiO_2 (in weight percent) for samples from the Crater Peak vent of Mount Spurr volcano, Alaska. Pre-1992 samples are discussed in Nye and Turner (1990). The plot also shows data from east (inverted triangles) and west (upright triangles) ancestral Crater Peak and the current Crater Peak (filled circles). Lines connecting symbols represent stratigraphic order, with the most siliceous end of each line being the oldest.

crease to the amount of fractionation. *If* the 1992 andesite was derived by simple fractional crystallization of the 1953 magma, then about 16 to 19 percent (by weight) of crystals would have to have separated and the concentrations of Rb should have increased to about 21 ppm, compared to the 15 ppm Rb in the 1992 andesite. The differences in Rb between 1953 and 1992 andesite are also unlikely to be have been produced by open-system processes such as fractionation combined with crustal assimilation, which also causes increasing Rb with increasing SiO_2.

Andesite from 1953 is also unlike 1992 andesite in its high Ti, Mg, Sc, Cr, and Ni. Some or all of this is to be expected because the 1953 andesite has lower SiO_2, and it is therefore less evolved.

TEPHRA

Tephra samples were analyzed in a search for compositional diversity in 1992 ejecta and to test for compositional differences between the light-colored (less dense) and dark-colored (more dense) tephra components (Neal and others, this volume). A more extended discussion is presented by Neal and others (this volume). The main conclusions are that all the light tephra and half of the dark tephra samples are identical to 1992 andesite in their concentrations of 10 major and 33 trace elements. Those dark tephra samples that are different have anomalously high Cs, Rb, and compatible transition metals including Cr and Ni. The anomalous compositions are the products of chemical heterogeneities on the scale of a few grams of material. When large masses (>50 grams) of carefully chosen lapilli were crushed together, the anomalous compositions were not found. The contaminant has not yet been identified, but it is not small fragments of the xenoliths discussed in the next section.

XENOLITHS

ALUMINOUS CORDIERITE- AND SILLIMANITE-BEARING XENOLITHS

1992 ejecta also include a minor proportion of xenoliths. These are partially fused metamorphic rocks with 60 to 70 percent SiO_2, which contain glass, plagioclase, and some combination of cordierite, sillimanite, garnet, biotite, pyroxene, and spinel. Their bulk compositions fall off the trend of Mount Spurr lavas toward high Ti, Fe, K, Cs, Rb, Ba, REE, Nb, Ta (but not Zr and Hf), Y, U, Th, Pb, V, Cr, and Ni and low Na, Ca, and Sr (table 3, figure 5). The bulk-xenolith composition may not reflect the composition of the protolith ,because the liquid (now glass) may have moved with respect to the crystal residue. Additional work on glass separates is in progress. The high transition metal concentrations and low Na make it unlikely that xenoliths such as these have been routinely

Table 3. Whole-rock compositions of selected metamorphic xenoliths from 1992 eruptions of Crater Peak vent, Mount Spurr, Alaska.

[Major elements normalized to 100 percent anhydrous. FeOt is total iron as FeO. Number of reported decimal places may exceed analytical precision.]

	Aluminous xenoliths												Siliceous xenoliths		
Sample #	92AMm 102D	92AMm 111A-1	92AMm 102F	92AMm 111A-2	92JES -05	92AMm 102A	92AMm 113B	92MHS 04a	92AMm 113A	92JES -09	92MHS 02a	92MHS 05b	92AMm 113D	92JES -02	92JES -04
	Major-elements, in weight percent														
SiO_2	50.34	60.15	61.03	62.34	63.17	64.66	65.02	65.39	65.83	67.55	68.38	69.19	76.46	76.17	75.74
TiO_2	1.33	101	0.87	0.92	0.88	0.87	1.02	0.84	0.84	0.77	0.79	0.75	0.00	0.02	0.02
Al_2O_3	2469	18.83	18.06	19.07	17.32	16.18	17.79	16.40	17.24	15.86	15.39	15.81	14.05	13.13	14.04
FeOt	6.83	8.57	7.65	7.20	7.81	6.77	6.73	5.96	6.63	5.82	6.07	4.40	0.57	0.71	0.48
MnO	0.06	0.19	0.24	0.28	0.16	0.15	0.11	0.12	0.14	0.13	0.13	0.09	0.02	0.07	0.03
MgO	3.68	3.81	3.34	3.33	3.71	2.88	2.51	2.96	2.44	2.85	221	2.12	0.00	0.01	0.00
CaO	7.95	2.08	2.66	1.75	1.94	2.96	1	3.04	1.99	2.05	1.91	2.34	1 . 1	3.20	1.91
Na_2O	3.75	2.45	2.90	2.73	1.99	2.92	2.13	2.24	2.64	2.16	2.28	2.21	7.11	5.85	6.47
K_2O	1.27	2.62	2.98	2.18	2.69	2.36	3.00	2.85	2.05	2.58	2.63	2.92	0.52	0.79	1.15
P_2O_5	0.10	0.29	0.25	0.20	0.33	0.27	0.19	0.20	0.21	0.23	0.23	0.16	0.18	0.06	0.16
	Traceelements, in parts per million														
Cs	0.47	4.48	5.76	1.94	3.10	3.02	4.46	2.74	2.40	2.79	2.57	3.45	0.20	0.17	0.26
Rb	30.84	81.65	115.4	55.98	83.47	71.48	85.48	69.42	66.81	76.72	75.99	68.82	9.75	13.26	22.79
Ba	1045	1231	1258	2174	791	944	883	837	760	773	931	679	58	154	174
Sr	793	221	236	153	228	304	231	296	229	216	243	282	45	123	116
La	15.35	29.95	27.64	27.82	26.79	24.57	27.45	23.35	26.88	23.82	24.46	22.76	1.75	2.54	3.48
Ce	25.31	56.93	54.39	46.72	51.80	46.29	52.98	44.43	51.04	45.27	46.79	43.42	3.33	4.60	6.40
Pr	2.78	6.38	6.34	6.21	5.72	5.44	6.21	5.25	6.00	5.26	5.54	5.11	0.35	0.51	0.69
Nd	11.31	25.66	26.04	25.60	23.14	22.64	26.15	21.22	24.52	21.75	22.80	20.84	1.04	1.85	2.51
Sm	2.06	5.83	5.92	5.49	5.22	4.98	6.70	4.79	5.70	4.76	5.36	4.72	0.39	0.50	0.67
Eu	2.2	1.26	1.1	1.04	1.39	1.44	1.29	1.17	1.42	1.22	1.39	1.23	0.02	0.17	0.17
Gd	2.53	5.04	5.74	5.27	4.58	4.71	6.49	4.38	5.00	4.46	5.06	4.02	0.29	0.50	0.53
Tb	0.26	0.82	0.9	0.85	0.80	0.77	1.16	0.72	0.90	0.76	0.88	0.68	0.08	0.10	0.08
Dy	1.47	4.74	5.33	5.01	5.19	4.62	6.95	4.41	5.59	4.60	5.37	3.96	0.49	0.52	0.45
Ho	0.3	0.94	1.09	1.04	1.13	0.98	1.43	0.91	1.16	0.93	1.14	0.81	0.09	0.10	0.08
Er	0.8	2.62	3.28	2.96	3.39	2.86	3.99	2.58	3.32	2.69	3.30	2.28	0.24	0.26	0.20
Tm	0.11	0.36	0.47	0.40	0.49	0.4	0.55	0.35	0.47	0.37	0.46	0.33	0.05	0.04	0.03
Yb	0.75	2.41	3.07	2.66	3.22	2.58	3.39	2.40	3.12	2.40	2.95	2.07	0.41	0.29	0.20
Lu	0.14	0.39	0.5	0.42	0.53	0.43	0.53	0.38	0.50	0.38	0.47	0.33	0.06	0.04	0.03
Y	7.87	23.08	29.5	22.77	31.32	26.29	35.80	25.09	28.01	25.41	30.94	21.77	2.71	3.45	2.78
Zr	190	170	145	171	149	149	209	152	153	136	155	160	44	31	33
Hf	3.75	4.68	3.37	3.87	4.05	4.02	5.01	4.17	4.17	3.59	4.15	4.28	2.28	1.13	1.14
Nb	8.97	12.23	12.02	8.39	12.22	11.4	12.04	10.57	9.12	10.30	10.21	9.50	2.26	3.44	3.49
Ta	0.64	0.81	0.84	0.59	0.77	0.69	0.87	0.71	0.61	0.76	0.61	0.65	0.40	0.70	0.90
Pb	4.23	12.69	14.12	16.13	13.53	14.2	11.67	8.87	9.74	12.43	11.89	11.77	10.18	9.20	10.37
Th	0.8	8.48	7.05	5.67	6.93	5.31	6.31	5.28	6.81	5.84	5.55	5.18	0.40	0.64	0.75
U	0.38	2.15	2.11	2.17	1.66	1.5	2.30	1.65	1.07	2.02	1.21	1.58	4.47	2.23	2.18
Ga	28	24	20	29	20	20	22	21	18	17	20	16	17	17	16
Cu	266	110	72	87	36	59	59	70	44	9	47	19	21	18	18
Zn	120	144	146	139	164	109	132	80	111	106	87	74	7	11	2
V	299	242	206	226	201	171	172	167	171	163	158	130	10	14	9
Sc	13	25	22	21	21	23	20	16	19	16	19	15	6	1	0
Cr	148	133	118	140	206	119	125	116	98	117	92	83	6	6	4
Ni	48	57	56	63	97	51	46	48	52	49	47	30	6	9	8

assimilated by Mount Spurr magmas. Nye and Turner (1990) appealed to a large-ion lithophile element (LILE)-rich, high-field-strength element (HFSE)- and heavy rare-earth element (HREE)-poor crustal contaminant in Spurr magmas. This component could logically be derived from small degrees of partial melting of country rock leaving such phases as garnet, spinel, zircon, and rutile in the residue. Whereas these xenoliths are not that component, their glass may be.

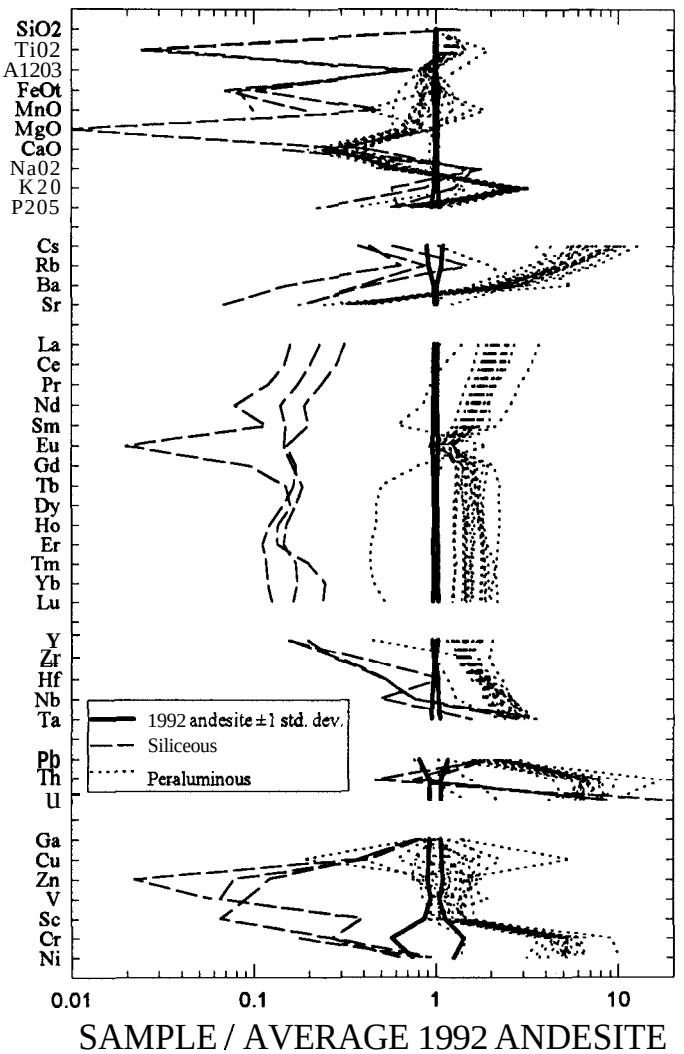

Figure 5. Compositions of aluminous and siliceous xenoliths compared to the mean composition of 1992 andesite. Each xenolith sample was normalized to the mean of all 1992 juvenile andesite blocks. FeO_t is total iron as FeO.

SILICEOUS XENOLITHS

A few siliceous, bright white, plagioclase-quartz-glass xenoliths of uncertain parentage also occur. They make up a very small percentage of erupted material. They have rhyolitic SiO_2 (table 3), but they are strongly depleted in all elements except Na, Rb, Ta, U, and Ni (fig. 5). Both mobile and immobile trace elements are depleted. Concentrations of K, Rb, Ba, Zr, and Y are all very low; they average around 0.8 percent, 17 ppm, 130 ppm, 36 ppm, and 2 ppm, respectively. For comparison, concentrations of these elements in Novarupta rhyolites, are 3.2 percent, 63 ppm, 900 ppm, 150 ppm, and 48 pprn (Hildreth, 1983; Nye, unpublished data). The siliceous xenoliths are unlikely to represent crustal minimum melts or any kind of a high-temperature crustal distillate, particularly because of their low LILE. The parents to these xenoliths may be some highly depleted protolith, such as hydrothermal veins, or they may be strongly leached rock of some other lithology. Xenoliths that are macroscopically similar to these are also found in prehistoric Crater Peak andesites.

REFERENCES CITED

Kienle J., Swanson, S.E., and Pulpan, H., 1983, Magmatism and subduction in the eastern Aleutian Arc, *in* Shimozuru, D., and Yokoyama, I., eds., Arc Volcanism: Physics and Tectonics: Terra Scientific Publishing Co. Tokyo, Japan, p. 191–224.

Nye, C.J., and Turner, D.L., 1990, Petrology, geochemistry, and age of the Spurr volcanic complex, eastern Aleutian arc: Bulletin of Volcanology, v. 52, p. 205–226.

Riehle, J.R., 1985, A reconnaissance of the major Holocene tephra deposits in the upper Cook Inlet region, Alaska: Journal of Volcanology and Geothermal Resources, v. 26, p. 37–74.

Wilson, F.H., Detterman, R.L., and Case, J.E., 1985, The Alaska Peninsula terrane: A definition: U.S. Geological Survey Open-File Report 85-450, 17 p.